Four-bar mechanism substitution for balance board experiments: a parametric study

Ambrus Zelei, Csenge A. Molnár and Tamás Insperger

Abstract Our research aims the study of balancing on a rolling balance board with respect to dynamic properties such as stability and stabilizability. The goal is to identify the parameter regions where human subjects are able to keep themselves stable in the upright position for at least 60 sec. The radius of the balance board and the height of the foot platform are adjusted for each individual test, which is a time demanding process.

We give a preliminary design of a substituting four-bar mechanism in order to speed up the balance board experiments and to extend the limits of the parameter study. The mechanism is tunable quickly in order to imitate the motion of the balance board with different radii and platform heights; whilst the agreement of the kinematic behaviour is almost perfect for tilt angles within the region of $\pm 30°$.

The dynamic behaviour of the mechanism and the balance board are compared based on theoretically derived stability diagrams associated with the underlying mechanical models. The balancing process is modelled by a proportional-derivative delayed feedback controller in order to account with the reaction time delay of the subject. We show that the stable parameter regions of the balance board and the mechanism are in good agreement, therefore the mechanism can be used as a substituting device for balance board.

Ambrus Zelei
MTA-BME Research Group on Dynamics of Machines and Vehicles and MTA-BME Lendület Human Balancing Research Group. Muegyetem rkp 3-5., Budapest, Hungary, H-1111, e-mail: zelei@mm.bme.hu

Csenge A. Molnár
Department of Applied Mechanics, Budapest University of Technology and Economics and MTA-BME Lendület Human Balancing Research Group, e-mail: csenge.molnar@mm.bme.hu

Tamás Insperger
Department of Applied Mechanics, Budapest University of Technology and Economics and MTA-BME Lendület Human Balancing Research Group, e-mail: insperger@mm.bme.hu

1 Introduction

Understanding the mechanism of keeping balance during everyday activities is an important task for physiologists and neuroscientists. Balance disorders often leads to falls, which may result in fatal injuries, especially in the elderly, therefore the development of techniques and biomechanical devices to prevent falling is of high importance [14, 15]. A key element of human balance research is to find an appropriate mechanical model with some adjustable characteristic parameters, which reflects balancing abilities of human subjects. For example, in stick balancing on the fingertip, the mechanical model is an inverted pendulum and the characteristic parameter is the smallest length of the stick that a subject is able to balance for certain time [2, 5, 6, 10, 18]. Typically, human subjects cannot balance stick of shorter than 30cm [11]. For quiet standing, the mechanical model is again an inverted pendulum [7, 16], however, the length of the pendulum, i.e., the height of the subject, is fixed and cannot be considered as an adjustable parameter. The advantage of the controlled inverted pendulum model is its publicity in the literature, e.g. [1, 4]. Balancing on a balance board is a generalized version of quiet standing, where some parameters of the balance board (e.g., the geometry or the mass) can be adjusted [3, 12]. Signals of balancing trials with different balance board geometry can be analyzed and quantified using the method of stabilometry [13, 17]. This way the ability of balancing in standing position can be analyzed as a function of some well defined parameters [12]. A drawback of such analysis is that the configuration of the balance board should be modified before each balancing trial, which, in case of systematic series of measurements, may be time-consuming. This motivates the idea of creating a simply adjustable mechanism, which provides the same motion as the balance board.

The concept of a four-bar mechanism substitution of a rolling balance board is proposed, which can speed up the balance board laboratory measurement process. The adjustment of the parameters of the balance board for different balancing trials takes considerable time. Especially the interchange of the arcs is time consuming, because in this case the balance board have to be completely disassembled (see Fig. 1/c). In addition to the quick adjustment, another advantage of the substituting mechanism is that the parameters can be adjusted continuously. The first goal of this work is to find the four-bar mechanism for which any point of the coupler link has the same trajectory as the corresponding point of the balance board. This ensures the same kinematic behavior. Secondly, it is shown that the dynamic behavior of the balance board and the mechanism under delayed feedback control is similar.

2 Kinematic analysis

The main criteria to the mechanism is that the ankle joint position of the balance board (see point A in Fig. 1/d) and the ankle joint position of the substituting mechanism (see point E in Fig. 2) must have the same trajectory when the tilt angle ϑ

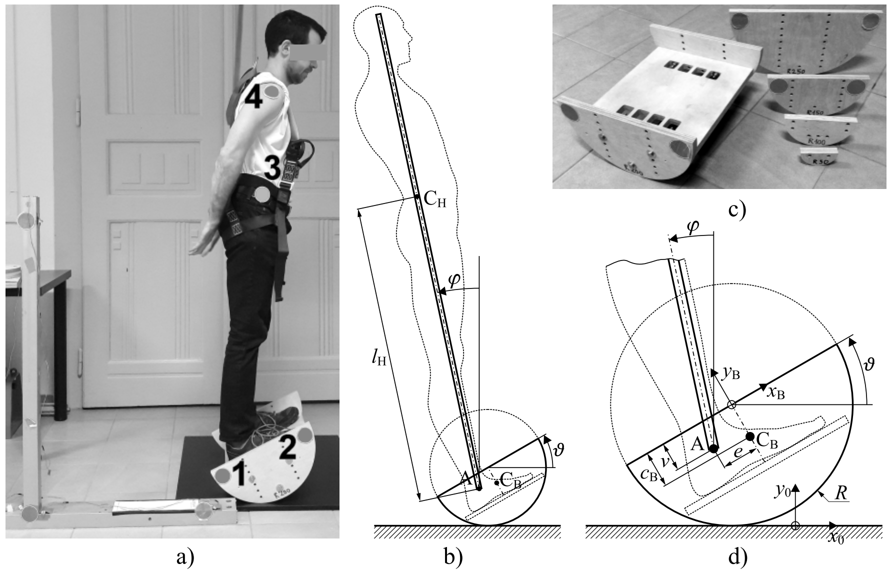

Fig. 1 Balance board experiment set-up (a), Simplified mechanical model (b), Balance board with interchangeable arcs (c), Geometry (d)

is varied. This results the same rigid body motion for the balance board and the coupler link of the mechanism.

2.1 Balance Board

A rolling balance board shown in Fig. 1 is tilted by angle ϑ with respect to the horizontal line. The subject's feet are placed on the balance board. The geometric parameters of the balance board are the radius R, the sole depth v and the parallel shift e. The location of the foot is given by e, which is a fix parameter for each subject, while R and v are tuned during balance experiments. Note that R and v can be adjusted to discrete values only. The human body is modeled by a rigid body of which the tilt angle φ is measured from the vertical.

Fig. 1/d introduces a global frame of reference denoted by 0 and a local frame B that is fixed to the balance board. The following position vector and rotation matrix provides the transformation between frames 0 and B:

$$ {}^{0}\mathbf{p}_{\mathrm{B}} = \begin{bmatrix} -R\vartheta \\ R \\ 0 \end{bmatrix}, \qquad {}^{0}\mathbf{R}_{\mathrm{B}} = \begin{bmatrix} c_\vartheta & -s_\vartheta & 0 \\ s_\vartheta & c_\vartheta & 0 \\ 0 & 0 & 1 \end{bmatrix}. \tag{1} $$

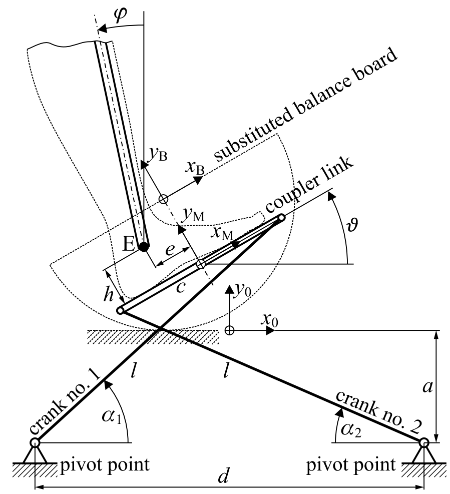

Fig. 2 Substituting four-bar mechanism

The position of the ankle joint A in the local and global system with the simplified notations $s_\vartheta = \sin\vartheta$ and $c_\vartheta = \cos\vartheta$ are given by:

$$^{\mathrm{B}}\mathbf{r}_{\mathrm{A}} = \begin{bmatrix} -e \\ -v \\ 0 \end{bmatrix}, \qquad ^{0}\mathbf{r}_{\mathrm{A}} = ^{0}\mathbf{R}_{\mathrm{B}}\, ^{\mathrm{B}}\mathbf{r}_{\mathrm{A}} + ^{0}\mathbf{p}_{\mathrm{B}} = \begin{bmatrix} -R\vartheta + v\, s_\vartheta - e\, c_\vartheta \\ R - v\, c_\vartheta - e\, s_\vartheta \\ 0 \end{bmatrix}. \quad (2)$$

2.2 Substituting mechanism

The geometric parameters of the four-bar mechanism shown in Fig. 2 are the distance d and the depth a of the pivot points, the crank lengths l, the coupler length c and the horizontal shift e of ankle joint E. The coupler link is tilted by angle ϑ, which angle corresponds to the tilt angle of the balance board. The foot is kept parallel to the coupler bar such that the elevation of the ankle joint is h.

2.2.1 Closed form solution for the crank angles

In order to express the ankle joint position, we need to determine the crank angles α_1 and α_2. The goal is to find α_1 and α_2 as functions of tilt angle ϑ such that the following vector-loop equations satisfy:

$$c_1 + c_2 = \frac{d}{l} + \frac{c}{l} c_\vartheta \quad (3)$$

$$s_1 - s_2 = \frac{c}{l} s_\vartheta, \quad (4)$$

where $s_1 = \sin\alpha_1$, $c_1 = \cos\alpha_1$, $s_2 = \sin\alpha_2$ and $c_2 = \cos\alpha_2$. The following identities are applied to reorganize the vector-loop equations:

$$c_1 + c_2 = 2c_p c_m \quad \text{and} \quad s_1 - s_2 = 2s_m c_p\,, \tag{5}$$

where $s_p = \sin\gamma_p$, $c_p = \cos\gamma_p$, $s_m = \sin\gamma_m$, $c_m = \cos\gamma_m$ and the new variables

$$\gamma_p = \frac{\alpha_1 + \alpha_2}{2}\,, \quad \text{and} \quad \gamma_m = \frac{\alpha_1 - \alpha_2}{2}\,. \tag{6}$$

Applying the identities (5) and the newly introduced variables (6), the vector-loop equations (3) and (4) can be reformulated again in the form

$$2c_p c_m = \frac{d}{l} + \frac{c}{l} c_\vartheta\,, \tag{7}$$

$$2s_m c_p = \frac{c}{l} s_\vartheta\,. \tag{8}$$

By dividing (8) and (7) the solution for γ_m and γ_p can be expressed as

$$\gamma_p = \arccos\left(\frac{c}{2l}\frac{s_\vartheta}{s_m}\right) \quad \text{and} \quad \gamma_m = \arctan\left(\frac{c\, s_\vartheta}{d + c\, c_\vartheta}\right)\,. \tag{9}$$

Finally, the crank angles are expressed using equations (6) as direct functions of the tilt angle ϑ:

$$\alpha_1 = \gamma_p + \gamma_m \quad \text{and} \quad \alpha_2 = \gamma_p - \gamma_m. \tag{10}$$

2.2.2 Position of the ankle joint in the global frame of reference

The position vector of the local frame of reference M can be written based on Fig. 2. Since the origin is in the middle of the coupler bar, the average of the endpoint positions of the cranks are used.

$$^{0}\mathbf{p}_{\mathrm{M}} = \begin{bmatrix} ^{0}x_{\mathrm{M}} \\ ^{0}y_{\mathrm{M}} \\ 0 \end{bmatrix} = \begin{bmatrix} \frac{1}{2}(-d + l\, c_1) + \frac{1}{2}(d - l\, c_2) \\ -a + \frac{1}{2} l\, s_1 + \frac{1}{2} l\, s_2 \\ 0 \end{bmatrix} = \begin{bmatrix} \frac{l}{2}(c_1 - c_2) \\ -a + \frac{l}{2}(s_1 + s_2) \\ 0 \end{bmatrix} \tag{11}$$

The fully expanded expressions for the position of the origin of frame M as functions of ϑ are

$$^{0}x_{\mathrm{M}} = -\frac{cA\, s_\vartheta}{2(d + c\, c_\vartheta)B}, \quad \text{and} \quad ^{0}y_{\mathrm{M}} = -a + \frac{A}{2B}, \tag{12}$$

where

$$A = \sqrt{4l^2 - c^2 - d^2 - 2cd\,c_\vartheta} \quad \text{and} \quad B = \sqrt{1 + \frac{c^2\,s_\vartheta^2}{(d + c\,c_\vartheta)^2}}\,. \tag{13}$$

Since the tilt angle ϑ are the same, the rotation matrix of reference frames 0 and M is the same as in the case of the balance board:

$$^0\mathbf{R}_\mathrm{M} = {}^0\,\mathbf{R}_\mathrm{B}\,. \tag{14}$$

Finally, the ankle joint E position in the local and the global frames are expressed as

$$^\mathrm{M}\mathbf{r}_\mathrm{E} = \begin{bmatrix} -e \\ h \\ 0 \end{bmatrix}, \qquad {}^0\mathbf{r}_\mathrm{E} = {}^0\,\mathbf{R}_\mathrm{M}\,{}^\mathrm{M}\mathbf{r}_\mathrm{E} + {}^0\mathbf{p}_\mathrm{M} = \begin{bmatrix} {}^0x_\mathrm{M} - h\,s_\vartheta - e\,c_\vartheta \\ {}^0y_\mathrm{M} + h\,c_\vartheta - e\,s_\vartheta \\ 0 \end{bmatrix}. \tag{15}$$

2.3 Optimization of the substituting mechanism

The cost function below expresses the integral of the error between the balance board and the substituting mechanism ankle positions, which have to be minimized:

$$\int\limits_{-\vartheta_\mathrm{max}}^{\vartheta_\mathrm{max}} \left|{}^0\mathbf{r}_\mathrm{E} - {}^0\mathbf{r}_\mathrm{A}\right|^2 \mathrm{d}\vartheta = \min! \tag{16}$$

The set of parameters $\{c,\, d,\, a,\, l,\, h\}$ of the substituting mechanism has to be found for which the cost function (16) is minimal in case of a certain set of parameters $\{R,\, v\}$ of the balance board. The number of unknown parameters is reduced by considering $\vartheta = 0$ horizontal position. Based on equations (2), (12), (13) and (15), expression ${}^0y_\mathrm{E} = {}^0y_\mathrm{A}$ reads:

$$R - v\,c_\vartheta - e\,s_\vartheta = -a + \frac{A}{2B} + h\,c_\vartheta - e\,s_\vartheta, \tag{17}$$

which simplifies after canceling the term $e\,s_\vartheta$ and substituting $\vartheta = 0$. Substituting expressions $B(\vartheta = 0) = 1$ and $A(\vartheta = 0) = A_0$ we obtain an expression for a:

$$a = v + \frac{A_0}{2} + h - R, \quad \text{with} \quad A_0 = \sqrt{4l^2 - c^2 - d^2 - 2cd}\,. \tag{18}$$

Parameter c can be fixed too by setting its value in a certain region found by trial-and-error method. Out of this region there is no solution that results close to zero cost function (16). We set $c = 1.4R$.

After fixing parameters a and c, the remaining unknown parameters are d, l and h. The minimum cost function have to be found in the three dimensional parameter space (d, l, h). By means of a well chosen initial guess and a local minimum search algorithm we construct generally applicable formulae for the substituting mechanism geometric parameters:

$$c = 1.4R\,; \quad d = 2.956R\,; \quad a = 0.8786R\,; \quad l = 2.530R\,; \quad h = 0.5896R - v \tag{19}$$

The above parameters of the substituting mechanism can be set according to the desired R and v values of the equivalent balance board. A few examples are collected in Table 1 and in Fig. 3. Note that parameter a does not play any role in a real application, because it induces a shift only of the ankle joint path and hence neither the gradient of the potential function nor the stability properties change. Fig. 3 shows that the ankle joint paths for the balance board and the mechanism overlap each other with a difference smaller than $1\,\mathrm{mm}$.

Table 1 Some examples for optimal parameters of the substituting mechanism (the parameter values used in the dynamic analysis in Section 3 are indicated by boldface)

balance board radius	$R = 0.1\mathrm{m}$	$R = \mathbf{0.25}\mathrm{m}$
parameter set for any v value		
coupler length	$c = 0.14\mathrm{m}$	$c = \mathbf{0.35}\mathrm{m}$
pivot points distance	$d = 0.2956\mathrm{m}$	$d = \mathbf{0.739}\mathrm{m}$
(pivot points depth)	$(a = 0.08786\mathrm{m})$	$(a = \mathbf{0.21965}\mathrm{m})$
crank length	$l = 0.253\mathrm{m}$	$l = \mathbf{0.6325}\mathrm{m}$
sole elevation for $v = \mathbf{-0.1}\mathrm{m}$	$h = 0.15896\mathrm{m}$	$h = \mathbf{0.2474}\mathrm{m}$
sole elevation for $v = 0\mathrm{m}$	$h = 0.05896\mathrm{m}$	$h = 0.1474\mathrm{m}$
sole elevation for $v = 0.1\mathrm{m}$	$h = -0.04104\mathrm{m}$	$h = 0.0474\mathrm{m}$

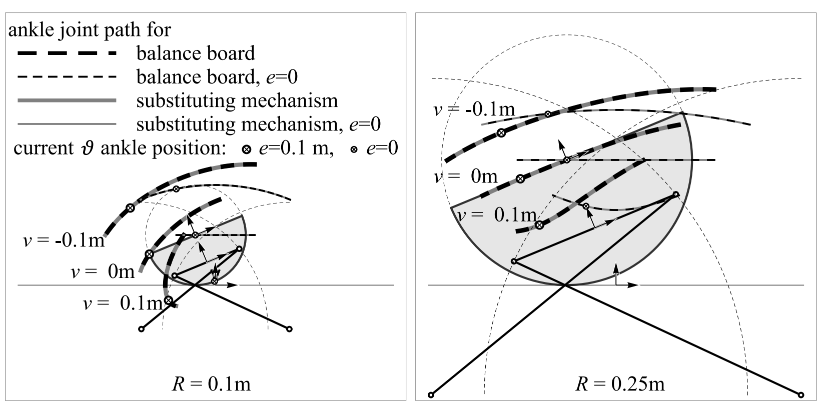

Fig. 3 Balance board and four bar mechanism together with parameters $R = 0.1\mathrm{m}$, $R = 0.25\mathrm{m}$ and $v = -0.1\mathrm{m}$, $v = 0\mathrm{m}$, $v = 0.1\mathrm{m}$

3 Dynamic analysis

We construct the dynamic model both for the balance board and the mechanism. The dynamic behaviour is compared via the mass and stiffness matrices and the stability properties. Since the kinematics (i.e. the motion of the ankle joint as the function of the tilt angle) are the same in case of both equipments, it is obvious that the dynamic behaviour is the same when the inertial parameters of the equipments are neglected (see Section 3.5). We observed that when considering the inertial parameters of the equipments, the mass and stiffness matrix and the stability behavior are still similar.

3.1 Dynamic model of a human standing on the balance board

The mechanical model depicted in Fig. 1/a is applied. We consider undeformable bodies and ground, therefore rolling resistance does not appear in the model. This is an acceptable simplification, since the balance board is placed on hard surface and the wooden made balance board itself is also stiff.

We apply the Lagrange equation of motion for which the kinetic energy T, the potential function U and the generalized force $\mathbf{Q}$ of the ankle control torque M are expressed as:

$$T = \frac{1}{2} m_{\mathrm{H}} \left|\dot{\mathbf{r}}_{\mathrm{C_H}}\right|^2 + \frac{1}{2} m_{\mathrm{B}} \left|\dot{\mathbf{r}}_{\mathrm{C_B}}\right|^2 + \frac{1}{2} J_{\mathrm{H}} \dot{\varphi}^2 + \frac{1}{2} J_{\mathrm{B}} \dot{\vartheta}^2 \,, \tag{20}$$

$$U = m_{\mathrm{H}}\, g\, y_{\mathrm{C_H}} + m_{\mathrm{B}}\, g\, y_{\mathrm{C_B}} + \frac{1}{2} k_{\mathrm{A}} \left(\vartheta - \varphi + \varphi_0\right)^2 \,, \tag{21}$$

$$\mathbf{Q} = \left[-M,\, M\right]^{\mathrm{T}} \,, \tag{22}$$

where m_{H} and m_{B} are the mass and J_{H} and J_{B} are the mass moment inertia of the human body and the balance board respectively, k_{A} is the stiffness of the ankle and $\varphi_0 = \arcsin(e/l_{\mathrm{H}})$ is the equilibrium angle of the human (Fig. 1/a shows the tilted human body near equilibrium). The human body and balance board centre of mass positions are simply given by $\mathbf{r}_{\mathrm{C_H}} = \mathbf{r}_{\mathrm{A}} + l_{\mathrm{H}} \left[-s_{\varphi},\, c_{\varphi},\, 0\right]^{\mathrm{T}}$ and $\mathbf{r}_{\mathrm{C_B}} = \mathbf{p}_{\mathrm{B}} - c_{\mathrm{B}} \left[-s_{\vartheta},\, c_{\vartheta},\, 0\right]^{\mathrm{T}}$ respectively.

Using the generalized coordinates $\mathbf{q} = [\varphi(t),\, \vartheta(t)]$, the following form of the Lagrange equation of motion is used:

$$\frac{\mathrm{d}}{\mathrm{d}t} \frac{\partial T}{\partial \dot{q}_i} - \frac{\partial T}{\partial q_i} + \frac{\partial U}{\partial q_i} = Q_i \,; \qquad i = 1,\, 2\,. \tag{23}$$

3.2 Dynamic model of a human standing on the substituting mechanism

The mechanical model in Fig. 2 is applied with frictionless joints and undeformable bodies. The kinetic energy and potential function of the substituting mechanism reads

$$T = \frac{1}{2} m_{\mathrm{H}} \, |\dot{\mathbf{r}}_{\mathrm{C_H}}|^2 + \frac{1}{2} m_{\mathrm{c}} |\dot{\mathbf{p}}_{\mathrm{M}}|^2 + \frac{1}{2} J_{\mathrm{H}} \dot{\varphi}^2 + \frac{1}{2} J_{\mathrm{c}} \dot{\vartheta}^2 + \frac{1}{2} J_l \dot{\alpha}_1^2 + \frac{1}{2} J_l \dot{\alpha}_2^2 \,, \tag{24}$$

$$U = m_{\mathrm{H}} \, g \, y_{\mathrm{C_H}} + m_l \, g \frac{l}{2} s_1 + m_l \, g \frac{l}{2} s_2 + m_{\mathrm{c}} g y_{\mathrm{M}} + \frac{1}{2} k_{\mathrm{A}} \left(\vartheta - \varphi + \varphi_0 \right)^2 \,, \tag{25}$$

where m_{c} is the mass and J_{c} is the mass moment of inertia with respect to the centre of mass of the coupler link. The crank mass is m_l and J_l is the mass moment of inertia of one crank with respect to the pivot point. The centre of mass of the human body is $\mathbf{r}_{\mathrm{C_H}} = \mathbf{r}_{\mathrm{E}} + l_{\mathrm{H}} \, [-s_\varphi, \, c_\varphi, \, 0]^{\mathrm{T}}$. The generalized force vector $\mathbf{Q}$ is the same as in (22).

3.3 Computation of ankle torques during human balancing

During the balancing process the brain collects information from the environment via the sensory organs and after processing sends signals to the muscles. This process takes a certain time, which is modeled as a delay in the feedback loop. Here, we assume a delayed linear feedback controller [16]. The ankle torque is calculated based on the deviation from the equilibrium state $\mathbf{q}_0 = [\varphi_0, \, 0]$ as follows

$$M = P_\varphi \left(\varphi(t-\tau) - \varphi_0 \right) + P_\vartheta \, \vartheta(t-\tau) + D_\varphi \, \dot{\varphi}(t-\tau) + D_\vartheta \, \dot{\vartheta}(t-\tau) \,. \tag{26}$$

3.4 Stability diagrams

The linearized equation of motion reads:

$$\mathbf{M}\ddot{\mathbf{q}}(t) + \mathbf{K}\dot{\mathbf{q}}(t) + \mathbf{S}\mathbf{q}(t) = \mathbf{P}\mathbf{q}(t-\tau) + \mathbf{D}\dot{\mathbf{q}}(t-\tau) \,. \tag{27}$$

The stability of (27) can be determined by the semidiscretisation method [8]. The stability of the system is represented in the space of the four control gains P_φ, D_φ, P_ϑ and D_ϑ. A projection of the stability diagrams to a fixed pair of P_φ and D_φ is shown in Figure 4.

3.5 Comparison of stability properties in an illustrative example

The coefficient matrices and the stable region are compared in four cases:

- case **BB0**: balance board dynamic model, b. board inertia neglected ($m_\mathrm{B} = 0$, $J_\mathrm{B} = 0$)
- case **Me0**: mechanism dynamic model, mechanism inertia neglected ($m_\mathrm{c} = 0$, $m_l = 0$),
- case **BB**: complete balance board dynamic model,
- case **Me**: complete substituting mechanism dynamic model.

It is important to note, that the dynamic models are still not singular, even in the case when we neglect the inertia of the balancing equipments. If the balance board kinematics were imitated by the mechanism exactly, cases **BB0** and **Me0** would provide exactly the same dynamic behaviour. When the inertia of the balancing equipment is also considered, then a slightly modified dynamic behaviour is expected, which is detailed in this section.

The balance board parameters were set to $R = 0.25\mathrm{m}$ and $v = -0.1\mathrm{m}$ and the corresponding geometric parameters of the substituting mechanism are collected in Table 1. The horizontal shift of the ankle joint is $e = 0.1\mathrm{m}$. The inertial parameters of the balance board are: $m_\mathrm{B} = 3.42\mathrm{kg}$ and $J_\mathrm{B} = 0.0298\mathrm{kg}/,\mathrm{m}^2$. The centre of mass position is given by $c_\mathrm{B} = 0.136\mathrm{m}$. The inertial parameters of the substituting mechanism are: $m_\mathrm{c} = 2\mathrm{kg}$, $m_l = 1.5\mathrm{kg}$ and the mass moments of inertia J_c and J_l are calculated by considering homogeneous and prismatic bars. The parameters of the bar that represents the human body are body mass $m_\mathrm{H} = 65\mathrm{kg}$, centre of mass distance from the ankle $l_\mathrm{H} = 1\mathrm{m}$, estimated mass moment of inertia with respect to the centre of mass $J_\mathrm{H} \approx 1/12\, m_\mathrm{H}\, n^2 = 16.21\mathrm{kg}\,\mathrm{m}^2$, where $n = 1.73\mathrm{m}$ is the height of the subject. Ankle stiffness is $k_\mathrm{A} \approx 0.91\, m_\mathrm{H}\, g\, n/2 = 501.9\mathrm{Nm/rad}$ [9]. The damping matrix and the coefficient matrices of the delayed terms are the same in all cases:

$$\mathbf{K} = \begin{bmatrix} 0 & 0 \\ 0 & 0 \end{bmatrix}\ ; \quad \mathbf{P} = \begin{bmatrix} -P_\varphi & -P_\vartheta \\ P_\varphi & P_\vartheta \end{bmatrix}\ ; \quad \mathbf{D} = \begin{bmatrix} -D_\varphi & -D_\vartheta \\ D_\varphi & D_\vartheta \end{bmatrix}\,. \tag{28}$$

The mass and stiffness matrices in cases **BB0** and **Me0** respectively are:

$$\mathbf{M} = \begin{bmatrix} 81.211 & 21.986 \\ 21.986 & 8.6125 \end{bmatrix} \mathrm{kg\,m}^2\,; \quad \mathbf{S} = \begin{bmatrix} -132.53 & -501.93 \\ -501.93 & 438.16 \end{bmatrix} \mathrm{Nm/rad}\,. \tag{29}$$

$$\mathbf{M} = \begin{bmatrix} 81.211 & 22.040 \\ 22.040 & 8.6506 \end{bmatrix} \mathrm{kg\,m}^2\,; \quad \mathbf{S} = \begin{bmatrix} -132.53 & -501.93 \\ -501.93 & 451.09 \end{bmatrix} \mathrm{Nm/rad}\,. \tag{30}$$

In cases **BB0** and **Me0**, the difference between the elements of the mass matrices of are less than 0.5% and less than 3% for the stiffness matrices. This difference is because the mechanism can not imitate exactly the balance board motion. The mass and stiffness matrices in cases **BB** and **Me** respectively are:

$$\mathbf{M} = \begin{bmatrix} 81.211 & 21.986 \\ 21.986 & 8.6870 \end{bmatrix} \mathrm{kg\,m}^2\,; \quad \mathbf{S} = \begin{bmatrix} -132.53 & -501.93 \\ -501.93 & 442.71 \end{bmatrix} \mathrm{Nm/rad}\,. \quad (31)$$

$$\mathbf{M} = \begin{bmatrix} 81.211 & 22.040 \\ 22.040 & 8.7337 \end{bmatrix} \mathrm{kg\,m}^2\,; \quad \mathbf{S} = \begin{bmatrix} -132.53 & -501.93 \\ -501.93 & 456.85 \end{bmatrix} \mathrm{Nm/rad}\,. \quad (32)$$

Comparing cases **BB0** and **BB** one can notice that M_{22} and S_{22} changes only with $\Delta M_{22}^{\mathrm{B}} = 0.0745\mathrm{kg\,m}^2$ and $\Delta S_{22}^{\mathrm{B}} = 4.55\mathrm{Nm/rad}$. Comparing cases **Me0** and **Me** one can notice that M_{22} and S_{22} changes only with $\Delta M_{22}^{\mathrm{M}} = 0.0831\mathrm{kg\,m}^2$ and $\Delta S_{22}^{\mathrm{M}} = 5,76\mathrm{Nm/rad}$. Since $\Delta M_{22}^{\mathrm{B}} \approx \Delta M_{22}^{\mathrm{M}}$ and $\Delta S_{22}^{\mathrm{B}} \approx \Delta S_{22}^{\mathrm{M}}$, we can conclude that adding the inertia of the balancing equipments changes the dynamic behaviour similarly. Therefore the mechanism is suitable for the substitution of the original balance board.

Fig. 4 shows the stability maps generated by the method explained in Section 3.4 for cases **BB0**, **Me0**, **BB** and **Me**. The stability maps differ slightly which leads to the conclusion again that the substituting mechanism can be used in laboratory experiments instead of the balance board.

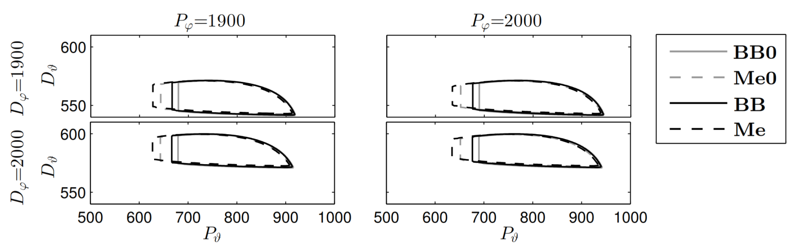

Fig. 4 Stability maps for the balance board and the substituting mechanism with and without neglecting the inertia of the balancing equipments (cases **BB0**, **Me0**, **BB** and **Me**).

4 Conclusions

We proposed the idea of a substituting mechanism that makes the balance board laboratory experiments faster and easier. The mechanism avoids the reassemble of the balance board in each measurement point regarding different parameter setting, like arc radius. Furthermore, the substitution mechanism can imitate the feeling of other balancing experimental equipments.

We have presented the geometric parameters of the mechanism that results the approximately the same kinematic behaviour as the balance board in the relevant tilt angle region. We showed that the dynamic properties of the balance board and the substituting mechanism are very close to each other so that the measurement result are not affected. The coefficients in the linearised equation of motion and the stable region of a controlled dynamic model were compared considering realistic inertial properties. We conclude that the application of a substituting mechanism is feasible.

References

1. Awrejcewicz, J., Wasilewski, G., Kudra, G., Reshmin, S.A.: An experiment with swinging up a double pendulum using feedback control. Journal of Computer and Systems Sciences International **51**(2), 176–182 (2012)
2. Cabrera, J., Milton, J.: Human stick balancing: tuning lévy flights to improve balance control. CHAOS **14**(3), 691698 (2004)
3. Chagdes, J., Rietdyk, S., Jeffrey, M., Howard, N., Raman, A.: Dynamic stability of a human standing on a balance board. journal of biomechanics. Journal of Biomechanics **46**(15), 2593–2602 (2013)
4. Enikov, E., Stépán, G.: Stabilizing an inverted pendulum - alternatives and limitations. Periodica Polytechnica - Mechanical Engineering **38**, 379–382 (1994)
5. Gawthrop, P., Loram, I., Gollee, H., Lakie, M.: Intermittent control models of human standing: similarities and differences **108**(2), 159–168 (2014)
6. Insperger, T., Milton, J.: Sensory uncertainty and stick balancing at the fingertip. Biological Cybernetics **108**(1), 85–101 (2014)
7. Insperger, T., Milton, J., Stepan, G.: Acceleration feedback improves balancing against reflex delay. Journal of the Royal Society Interface **10**(79), Article No. 20120,763 (2013)
8. Insperger, T., Stepan, G.: emi-discretization for time-delay systems Stability and Engineering applications. Springer, New York (2011)
9. Loram, I., Lakie, M.: Direct measurement of human ankle stiffness during quiet standing: the intrinsic mechanical stiffness is insufficient for stability **545**, 1041–1053 (2002)
10. Mehta, B., Schaal, S.: Forward models in visuomotor control. Journal of Neurophysiology **88**, 942953 (2002)
11. Milton, J., Meyer, R., Zhvanetsky, M., Ridge, S., Insperger, T.: Control at stability's edge minimizes energetic costs: expert stick balancing. J. Royal Soc. Interface **13**, 20160,212 (2016)
12. Molnar, C.A., Zelei, A., Insperger, T.: Estimation of human reaction time delay during balancing on balance board. In: Proceedings of International Conference on Biomedical Engineering (BioMed 2017), pp. 195–199. IASTED - ACTA Press (2017)
13. Nagymáté, G., R.M., K.: Stabilometry as a diagnostic tool in clinical medicine. Periodica Polytechnica, Mechanical Engineering **60**(4), 238–246 (2016)
14. Priplata, A., Niemi, J., Harry, J.D., Lipsitz, L.A., Collins, J.J.: Vibrating insoles and balance control in elderly people. Lancet **362**, 11231124 (2003)
15. Robinovitch, S., Feldman, F., Yang, Y., Schonnop R. Leung, P., Sarraf, T., Sims-Gould, J., Loughin, M.: Video capture of the circumstances of falls in elderly people residing in long-term care: an observational study. Lancet **381**, 47–54 (2013)
16. Stepan, G.: Delay effects in the human sensory system during balancing. Transactions of the Royal Society A **367**(1981), 1195–1212 (2009)
17. Terekhov, Y.: Stabilometry as a diagnostic tool in clinical medicine. Canadian Medical Association Journal **115**(7), 631–633 (1976)

18. Yoshikawa, N., Suzuki, Y., Kiyono, K., Nomura, T.: Intermittent feedback-control strategy for stabilizing inverted pendulum on manually controlled cart as analogy to human stick balancing. Frontiers in Computational Neuroscience **10**, 34 pages (2016)